Distributed Control Strategy Based on a Consensus Algorithm for the Inter-cell and Inter-cluster Voltage Balancing of a Cascaded H-Bridge Based STATCOM

Claudio Burgos-Mellado
Department of Electrical Engineering
University of Nottingham
Nottingham, UK
claudio.burgosmellado1@nottingham.ac.uk

Joseph Gutierrez
Department of Electrical Engineering
University of Chile
Santiago, Chile
joseph.gutierrez@ug.uchile.cl

Cristian Pineda
Department of Electrical Engineering
University of Nottingham
Nottingham, UK
ezxcp2@exmail.nottingham.ac.uk

Felipe Donoso
Department of Electrical Engineering
University of Nottingham
Nottingham, UK
ezxfd2@exmail.nottingham.ac.uk

Alan Watson
Department of Electrical Engineering
University of Nottingham
Nottingham, UK
alan.watson@nottingham.ac.uk

Mark Sumner
Department of Electrical Engineering
University of Nottingham
Nottingham, UK
mark.sumner@nottingham.ac.uk

Roberto Cardenas
Department of Electrical Engineering
University of Chile
Santiago, Chile
rcardenas@ing.uchile.cl

Andres Mora
Department of Electrical Engineering
Universidad Técnica Federico Santa María, Santiago, Chile
andres.mora@usm.cl

***Abstract*— Cascaded H-bridge converters are widely used in the implementation of medium voltage static synchronous compensators (STATCOMs). This is because of the advantages of relatively high-power density and the improved utilisation of low-voltage semiconductor devices. Major concerns with this topology are (i) to ensure a proper balance of the individual DC capacitor voltage in its cells, and (ii) the balancing of the average DC voltage between its clusters. In the research literature, these issues are typically addressed by using centralised control approaches, meaning that both an extensive processing capability and multiple digital outputs and communication channels for the switching signals are required, increasing system complexity. In contrast to this trend, in this paper, a distributed control scheme based on a consensus algorithm is proposed to deal with these issues in a three-phase STATCOM based on a cascaded H-bridge converter. The main advantages of the proposed control scheme are: (i) it does not require a centralised controller, since the cells work autonomously in a cooperative fashion to achieve voltage regulation, distributing the control effort among the cells, and (ii) it increases the fault tolerance of the converter and thus, the reliability of the system by adequately considering its redundancy. Extensive simulation work is provided to validate this proposal, and the characteristics described above.**

Keywords—STATCOM, Distributed Control System, Consensus Algorithm, Voltage Balancing, Modular multilevel-cascaded converter.

I. INTRODUCTION

The Cascaded H-Bridge (CHB) multilevel converter, illustrated in Fig. 1, also known as Single-Star Bridge-Cells (SSBC) [1], is one of the most utilised topologies for STATCOM applications. As depicted in Fig. 1, this topology considers three clusters composed of cascade-connected H-bridge cells. The fundamental challenge of this topology is the control of every floating capacitor voltage to the desired voltage level. To this end, the control of the floating capacitor voltages is typically addressed into two-stage, the balancing of the average value of the cluster capacitor voltages (inter-cluster) and the balancing of the capacitor voltages belonging to the same cluster (inter-cell). Traditionally, these concerns have been addressed in the literature by using centralised control schemes. This means that all the quantities (capacitor voltages, currents, etc.) required for implementing the control systems of the converter are sent to a central controller, in charge of processing all this information and controlling the power converter [1]. However, in recent years, distributed control approaches have been studied intensively (e.g. [2]). In this case, a centralised controller is not necessary owing to the control effort is distributed along with the cells of the converter, as shown in Fig. 1. Under this distributed approach, the cells of the converter can operate cooperatively to obtain global objectives such as the inter-cell and inter-cluster voltage balancing schemes. This approach has the following advantages: better reliability, flexibility, scalability, plug-and-play operation, and tolerance to single-point failures [3].

Some papers have proposed the use of the distributed approach to control modular multilevel cascade converters (MMCC) [2] [4] [5] [6] [7] [8]. In [2], a hybrid communication topology is implemented for a CHB-based STATCOM. The inverter is controlled using a distributed strategy. The main advantage of [2] is the use of parallel connections among cell in the communication network. By doing this, it is possible to reduce the transmission delay compared with a series communication network connection. In [4] [5], a distributed capacitor voltage strategy is presented and simulated for a Modular Multilevel Converter (M2C), in this case, to reduce the computational burden, the balancing algorithm sort groups of cells rather than individual cells. Then an inner control system sorts the cell within each group. In this case, the energy balance among arms is realised using a PI controller that

regulated the mean total energy among each arm. In [6], a distributed control strategy is implemented for a modular multilevel matrix converter (M3C). In this case, the outer voltage control loop that regulates the total mean energy among the nine arms is implemented in a master control system, using the double $\alpha\beta 0$ transformation. Then, the inner current control and balancing control of each cell is implemented in several slave controllers for each cell. Since this control scheme uses several slave controllers, the demand for communication speed is reduced, and a low cost CAN bus with a baud rate of only 1Mb/s is enough. Therefore, the communication burden is reduced, and system stability also gets improved. In [7], a distributed control technique for CHBs is presented. In this case, two different slave controls are defined to reduce the computational burden. The first one oversees the capacitor voltage balance of each cell, while the second one regulates the phase current. These two control systems are independent, and consequently, the communication network is reduced. In [8], a separate hybrid current controller for each cell of a STATCOM is proposed. A ring communication network is used to establish a communication link among the cells. The hybrid controller proposed in [8] allows controlling the STATCOM in a distributed manner. The performance of the proposal is evaluated under fault conditions, showing a good performance.

Within the research on distributed control schemes, the cooperative control, based on the consensus theory, has been successfully utilised and tested for microgrid (MG) applications. This theory has been used for addressing the following issues: (i) improvement of the sharing of reactive power [3] [9], (ii) optimal dispatch of distributed generation units in the MG [10] [11], and (iii) improvement of the power quality in unbalanced and/or distorted MGs [12] [13] [14] [15]. However, its use in the context of modular multilevel converters has not been extensively explored. To the best of the authors' knowledge, only [16] has proposed the use of a the consensus algorithm for a modular multilevel converter. In [16], the control the capacitor voltages in the cells of an MMC converter is designed and implemented using consensus theory. Experimental validation shows a good performance of the proposed approach. However, the performance of the distributed controller in front of a cell failure, time delays in the communication network, and failures in the communication links were not studied.

Based on the successful use of consensus-based distributed control schemes in the MG context, in this paper, the use of this approach to achieve the balancing of individual cells' voltage and the average DC capacitor voltage among the clusters in the STATCOM shown in Fig. 1, is proposed. In contrast to the scheme proposed in [16], where just a consensus scheme is proposed for individual cell balancing, this paper proposes a consensus-based distributed control scheme for voltage balancing in both the cells and the clusters of a CHB-based STATCOM. Moreover, an extensive simulation work is done to verify the performance of the proposal for the following scenarios: (i) the effects of a failure in a cell, (ii) the impact of communication time delays in the communication network, and (iii) the effects of communication link failures.

The rest of this paper is organised as follows: in section II, an overview of the consensus theory is presented. In section III, the proposed consensus algorithm and its implementation are discussed. Section IV presents the simulation results, and section V presents the conclusions of this work.

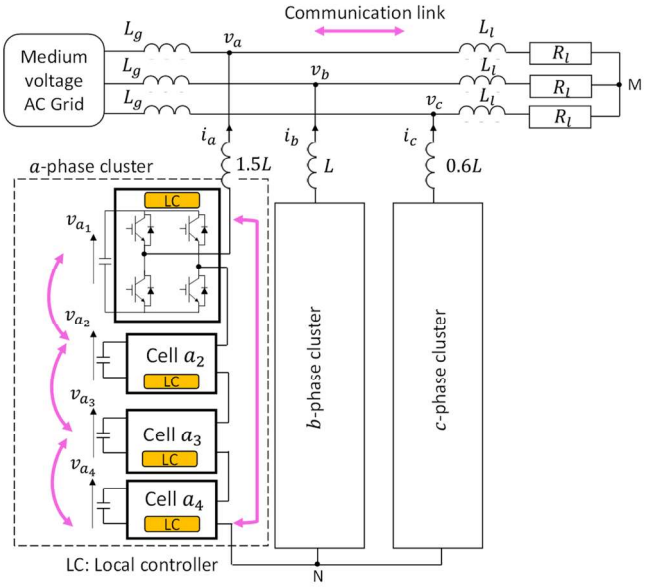

Fig. 1. CHB-based STATCOM under a distributed control system.

II. Proposed Approach

A. Communication Structure and Consensus Algorithm

A distributed communication network is required for the implementation of the proposed distributed cooperative control scheme. The bidirectional network considered in this work is modelled as an undirected graph $\mathbb{G} = (\mathcal{N}, \xi, A)$ among the cells $\mathcal{N} = \{1, \dots, N\}$, where ξ is the set of communication links and A is the non-negative $N \times N$ weighted adjacency matrix. The elements of A are $h_{ij} = h_{ji} \geq 0$, with $h_{ij} > 0$ if and only if $\{i, j\} \in \xi$ [17]. In this sense, let consider the case where all the N nodes of the graph $\mathbb{G}$ have scalar first-order single-integrator dynamics:

$$\dot{x}_i = u_i \tag{1}$$

where x_i and $u_i \in \mathbb{R}$. Also, let assumes that x_i denotes the value of some quantity of interest at node i. It is said that the variables x_i achieve consensus if $[x_i(t) - x_j(t)] \to 0$ as $t \to \infty$. Therefore, the consensus can be achieved via a feedback loop by applying the protocol u_i given by (2) [18] [19]. This control is distributed in that it only depends on the immediate neighbours $j \in \mathcal{N}(i)$ of node i in the graph topology. This protocol is known as a local voting protocol [18] [19].

$$u_i = -\frac{1}{k_i} \sum\nolimits_{j \in \mathcal{N}(i)} h_{ij} \cdot (x_i - x_j) \tag{2}$$

When the consensus is achieved, the quantity of interest x_i of each node of the system will be equal to each other and they will converge to the average of the initial states $x_i(0)$ as follows [18] [19]:

$$\lim_{t \to +\infty} x_i(t) = \lim_{t \to +\infty} x_j(t) = \frac{1}{N} \sum_{k=1}^{N} x_k(0) \tag{3}$$

It is worth to highlight that the consensus of variables x_i is achieved if and only if the graph $\mathbb{G}$ is a spanning tree [18] [19].

In (2), parameters h_{ij} are associated with the distributed communication network, whereas k_i is a gain that modifies the transient behaviour of the controller [17] [20]. Fig. 2 shows the consensus-based distributed controller.

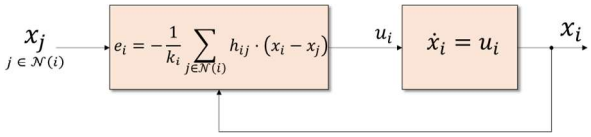

Fig. 2. Consensus-based distributed controller.

B. Relation Between Consensus Theory and the Typical Control System for Inter-Cell Voltage Balancing

In the operation of the CHB-based STATCOM, two control systems are used for capacitor voltage balancing purposes. The first one is for achieving the inter-cells voltage balancing (see Fig. 3), whereas the second one aims to balance the average DC voltage between the clusters of the converter (see Fig. 4). In both cases, proportional controllers are used (see Fig. 3 and Fig. 4, respectively). Also, it must be noted that the plants associated with each control loop have the form given by (1), i.e., they are integrative plants. [21]

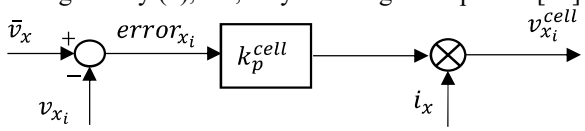

Where $i = 1, \dots, N$ and $x = a, b, c$

Fig. 3. Control system for inter-cell voltage balancing.

In Fig. 3, the typical control scheme for inter-cell voltage balancing for the CHB-based STATCOM is depicted. As seen, the cell average voltage $\bar{v}_x$ in cluster "x" is calculated and used as the reference value of every cell associated with that cluster. A proportional controller is used to drive the voltage in each cell of the cluster (v_{x_i}) to the reference value $\bar{v}_x$. Finally, the output of this controller is multiplied by the line current in that cluster i_x, producing a voltage variation $v_{x_i}^{cell}$ for each cell of the cluster "x", which is added to the output of the overall balance loop.

From Fig. 3, the error signal is determined as:

$$error_{x_i} = \bar{v}_x - v_{x_i} = \frac{1}{N}\sum_{j=1}^{N}\left(v_{x_j}\right) - v_{x_i} \tag{4}$$

The previous equation can be rewritten as:

$$error_{x_i} = \frac{\sum_{j=1}^{N}\left(v_{x_j}\right) - N v_{x_i}}{N} = \frac{1}{N}\sum_{j=1}^{N}\left(v_{x_j} - v_{x_i}\right) \tag{5}$$

By using (5) and taking into account the control scheme shown in Fig. 3, the final voltage variation $v_{x_i}^{cell}$ for each cell of cluster "x" is given by:

$$v_{x_i}^{cell} = -\frac{k_p^{cell}\cdot i_x}{N}\sum_{j=1}^{N}\left(v_{x_i} - v_{x_j}\right) \tag{6}$$

Thus, the power flow generated by the inter-cell control can be expressed as:

$$P_{x_i}^{cell} = i_x \cdot v_{x_i}^{cell} = -\frac{k_p^{cell}\cdot i_x^2}{N}\sum_{j=1}^{N}\left(v_{x_i} - v_{x_j}\right) \tag{7}$$

Finally, based on (6), it can be concluded that the inter-cell capacitor voltage control loop shown in Fig. 3 can be represented by the consensus form given by (2). Thus, the inter-cell voltage balancing can be performed in a distributed manner.

C. Relation Between Consensus Theory and the Typical Control System for Inter-Cluster Voltage Balancing

Fig. 4 shows the inter-cluster voltage balancing control loop of the converter. Note that this control system uses $\bar{v}_C$ as reference, which is calculated as the average of the DC voltage of the three clusters that composed the STATCOM. A proportional controller is used to control the cluster voltage v_{Cx} to $\bar{v}_C$ [21]. The output of the controller is multiplied by the line current i_x, producing the control action v_{Cx}^{cl} to regulate the inter-cluster DC voltages.

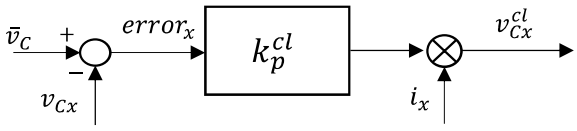

Where $x = a, b, c$

Fig. 4. Control diagram for inter-cluster voltage balancing. The variable v_{Cx} correspond to the average DC voltage in cluster x.

In Fig. 4, the average cluster voltage $\bar{v}_C$ is calculated as (8). In this equation, v_{Cj} (with $j = 1, 2, 3$) corresponds to the average DC voltage in each cluster, calculated as the average of the voltages of the capacitors of the cells in that cluster.

$$\bar{v}_C = \frac{1}{3}\sum_{j=1}^{3} v_{Cj} \tag{8}$$

In this case, considering that $v_{C_1} = v_{Ca}$, $v_{C_2} = v_{Cb}$ and $v_{C_3} = v_{Cc}$ the error signal can be expressed as

$$error_x = \bar{v}_C - v_{Cx} = \frac{1}{3}\sum_{j=1}^{3}\left(v_{Cj}\right) - v_{Cx} \tag{9}$$

Analogously, the error signal can be rewritten as

$$error_x = \frac{1}{3}\sum_{j=1}^{3}\left(v_{Cj} - v_{Cx}\right) \tag{10}$$

Based on the above equation, the final signal v_{Cx}^{cl} for achieving the inter-cluster voltage balancing in the STATCOM is given by:

$$v_{Cx}^{cl} = -k_p^{cl}\cdot\frac{i_x}{3}\sum_{j=1}^{3}\left(v_{Cx} - v_{Cj}\right) \tag{11}$$

Finally, the power flow generated to achieve the inter-cluster voltage balancing is given by:

$$P_{Cx}^{cl} = i_x \cdot v_{Cx}^{cl} = -k_p^{cl}\cdot\frac{i_x^2}{3}\sum_{j=1}^{3}\left(v_{Cx} - v_{Cj}\right) \tag{12}$$

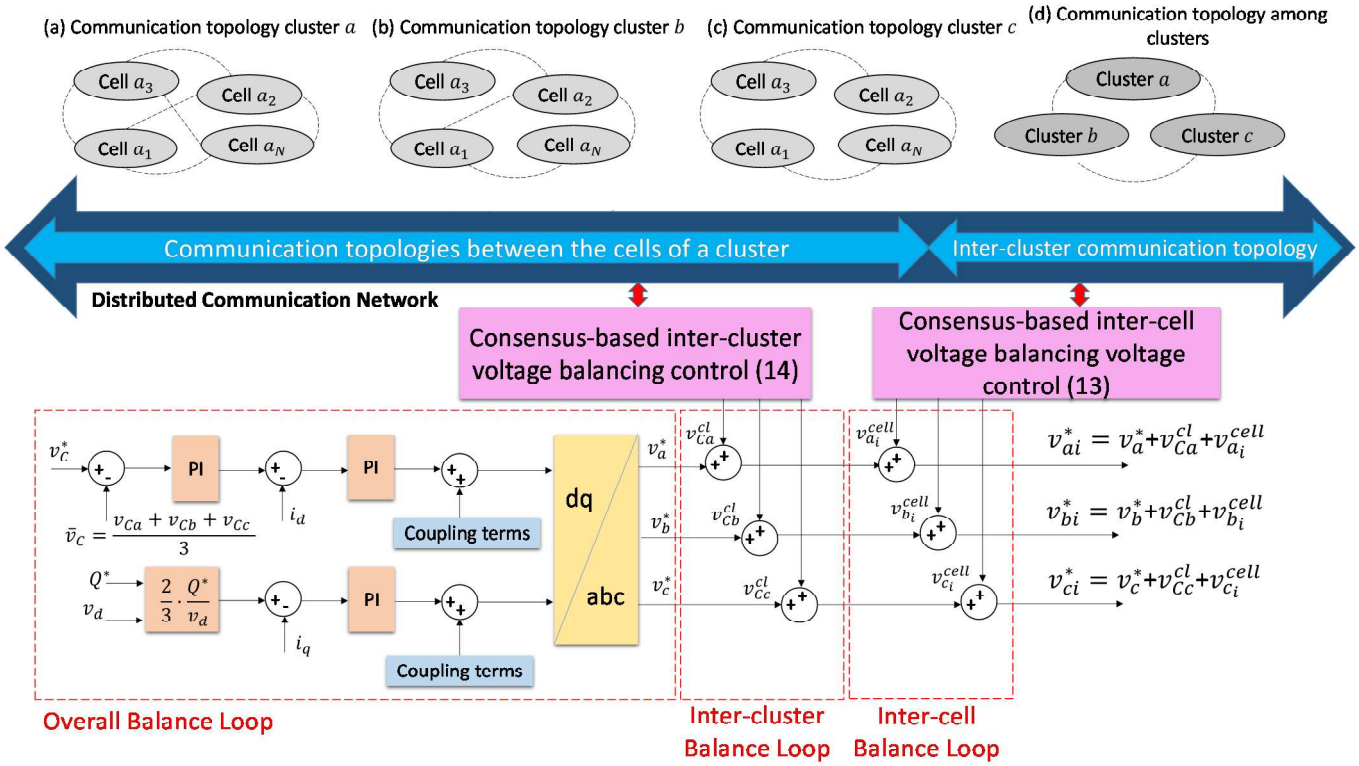

Fig. 5. Proposed Consensus-based distributed control scheme for inter-cluster and inter-cell balancing.

Similar to the inter-cell voltage balancing control loop discussed in the section II-B, in this section, it is demonstrated that the typical control loop for balancing voltage between clusters (see Fig. 4) can be expressed in terms of a consensus algorithm. This means that the inter-cluster voltage control in the CHB-based STATCOM can also be performed through a distributed approach.

III. Proposed Consensus-Based Control System for the Inter-Cell and Inter-Cluster Voltage Balancing

In the previous section, it was demonstrated that both the inter-cell and inter-cluster capacitor voltage balancing control loops depicted in Fig. 3 and Fig. 4 can be written in terms of a consensus algorithm (2). In particular, the inter-cell controller can be implemented by using the consensus algorithm (6). Moreover, the inter-cluster controller can be implemented via the consensus algorithm (11). Note that so far, (6) and (11) do not consider the communication topology between the elements of the system (adjacency matrix in (2)). To do that, let consider a graph $\mathbb{G}$ as that defined in section II-A. For the inter-cell consensus algorithm (6), the graph $\mathbb{G}$ is defined as follows: a graph where the cells of a particular cluster are the vertices and the communications links among them are the edges. Examples of possible graphs are depicted on the top of Fig. 5 (graphs (a)-(c)). In this figure, if the controller uses the graph (a) means that the average of all cells of the cluster is considered. On the other hand, if graph (b) is used, means that the controller taking into account the average of a portion of the voltages of the cells that composed that cluster. Finally, if the graph (c) is considered, it means that the controller is taking the average of just the neighbouring cells voltage.

In a similar way, graph (d) shown on the top of Fig. 5 shows a communication topology that can be used to implement the inter-cluster consensus algorithm (11).

Finally, the consensus algorithms (6) and (11), considering a distributed communication network, look like (13) and (14) respectively. It worth remembering that h_{ij} in (13) represents the elements of the adjacency matrix (A_{cell}) used to model the inter-cell communication topology. Similarly, g_{xj} are the elements of the inter-cluster adjacency matrix ($A_{cluster}$).

$$v_{x_i}^{cell} = -\frac{k_p^{cell} \cdot i_x}{N} \sum_{j=1}^{N} h_{ij} \cdot \left(v_{x_i} - v_{x_j}\right) \tag{13}$$

$$v_{Cx}^{cl} = -k_p^{cl} \cdot \frac{i_x}{3} \sum_{j=1}^{3} g_{xj} \cdot \left(v_{Cx} - v_{Cj}\right) \tag{14}$$

It should be highlighted that in this paper unless otherwise stated, the inter-cell communication topology is that represented by the graph (a) (see on the top of Fig. 5), thus A_{cell} is given by (15). Moreover, the communication topology used to implement the inter-cluster distributed controller is that given by graph (d) (see the top of Fig. 5), being (16) the mathematical representation of the adjacency matrix $A_{cluster}$. It should be noted that gain of (13) and (14) are time-variant because the line current i_x is a periodic quantity. However, as is discussed in [16], these gains only affect the convergence time of the controller [20], and they will not impact the consensus.

$$A_{cell} = \begin{bmatrix} h_{11}=0 & h_{12}=1 & h_{13}=1 & h_{14}=1 \\ h_{21}=1 & h_{22}=0 & h_{23}=1 & h_{24}=1 \\ h_{31}=1 & h_{32}=1 & h_{33}=0 & h_{34}=1 \\ h_{41}=1 & h_{42}=1 & h_{43}=1 & h_{44}=0 \end{bmatrix} \quad (15)$$

$$A_{cluster} = \begin{bmatrix} g_{11}=0 & g_{12}=1 & g_{13}=1 \\ g_{21}=1 & g_{22}=0 & g_{23}=1 \\ g_{31}=1 & g_{32}=1 & g_{33}=0 \end{bmatrix} \quad (16)$$

The implementation of the proposed consensus-based distributed controller is depicted in Fig. 5. In this scheme, three control systems can be identified. The controller labelled as overall balance loop is in charge of controlling the reactive power (Q^*) injected by the STATCOM to the system and to perform an overall voltage control [22]. The inter-cluster control loop aims to regulate the mean-DC voltage among the clusters of the STATCOM. The inter-cell controller regulates the individual DC-voltage in each capacitor of each cluster. Finally, the output signals cluster ($v_{ai}^*, v_{bi}^*, v_{ci}^*$ for clusters a, b and c respectively) of this control system are sent to the modulation stage, where the phase-shift PWM technique is used [23].

IV. Simulation Results

In this section, the performance of the proposed control scheme shown in Fig. 5 is evaluated. To do this, the system depicted in Fig. 1 is simulated by using PLECS software, with the parameters displayed in TABLE I. The performance of the proposed controller is verified for the following scenarios: (i) performance of the control system front of a cell failure, (ii) the effects of communication time delays in the communication network, and (iii) performance of the controller in front of failures on the communication links. It should be highlighted that for the simulation tests shown in this section unless otherwise stated; the inter-cell communication topology is that represented by the graph (a) (see the top of Fig. 5). Equation (15) shows the adjacency matrix (A_{cell}) associated with this graph. Similarly, the communication topology used to implement the inter-cluster distributed controller is that given by the graph (d) (see the top of Fig. 5). Equation (16) shows the mathematical representation of this matrix.

TABLE I. System parameters.

Parameter	Symbol	Value
Switching frequency	f_{sw}	1kHz
Cell capacitance	C	$5mF \pm 1\%$
Grid frequency	ω_g	$2\pi \cdot 50$
Grid inductance	L_g	5mH
Grid voltage (peak to peak)	V_{p-p}	10kV
Number of cells per cluster	N	4
Load Resistance	R_l	50Ω
Load Inductance	L_l	1mH
Arm inductance	L	10mH
Inter-cell control gain	k_p^{cell}	0.3
Inter-cluster control gain	k_p^{cl}	0.01
STATCOM power rating	S	10MVA
DC reference voltage	v_C^*	3750V

A. Test scenario 1: Performance of the distributed controller in front of a cell failure

In this test, the performance of the proposed distributed control scheme is evaluated. In particular, a failure (a short circuit) in the cell a_4 (see Fig. 1) is emulated. In this case, cell a_4 is bypassed. Thus, the a-phase cluster continues working with just three cells after the failure. Four steps are considered in this test: step 1 (0s⩽t<5s), where only the overall balance control loop is working to regulate the reactive power at Q^*=10MVar and v_C^* at 3750V; step 2 (5s⩽t<10s), where the proposed inter-cell control loop is enabled (see Fig. 5). In step 3 (10s⩽t<15s), the inter-cluster control loop is enabled to achieve an equal mean DC voltage among the cluster of the STATCOM. Finally, at the beginning of step 4 (15s⩽t<20s) a failure in cell a_4 is emulated, thus, that cell is bypassed.

Fig. 6(a) shows the voltage in each one of the twelve cells that compose the STATCOM of Fig. 1 during the four steps studied in this work. In step 1, it can be noted that these voltages are not equal due to the different capacitances used and their unequal initial voltages: if these voltages are not controlled, they will diverge until the system becomes unstable. At the beginning of step 2 (and onwards), this trend is changed, and now, the cell voltages are regulated in each cluster. Note in step 2 that, the cell voltages in a particular cluster reach a different convergence voltage compared with the other clusters because the STATCOM is connected to the system through unequal line impedances, which produce unbalanced voltages at its output. This behaviour is shown in steps 1-2 depicted in Fig. 6 (b), where the mean DC voltage of each cluster is depicted (during the whole test). Indeed, in steps 1 and 2 (when the consensus algorithm (14) is disabled), there is an unequal average DC voltage among the clusters. This is overcome, at the beginning of step 3 (and onwards), where the proposed inter-cluster control loop is working. In step 3 of Fig. 6 (a)-(b), both consensus algorithms are working, and it can be concluded that they are effective for balancing both cell and cluster voltages of the STATCOM. In this situation, at the beginning of step 4 (t=15s), a failure of cell a_4 is emulated. In this test, it can be concluded that despite this critical scenario, the inter-cell and inter-cluster voltage balancing is continuously achieved by the proposed control scheme (see Fig. 5). In step 4 of Fig. 6(a), the three cells in the a-phase cluster reach a higher convergence voltage than that achieved in step 3. This is because these cells have to supply the voltage that was provided by cell a_4 before its failure. Note that in this case, the proposed consensus algorithms autonomously calculate a new operating point in the cells of the STATCOM to achieve the consensus aims.

It should be noted that in this scenario (step 4), the STATCOM continues injecting the reactive power references (Q^*=10MVar) to the system, as shown in Fig. 7. It should be pointed out that in step 4, it was assumed that the STATCOM has cell redundancy in its clusters.

Finally, Fig. 8 and Fig. 9 show the voltage at the output of the STATCOM for step 3 and step 4, respectively. It worth remembering that during step 4, the cluster "a" is composed just by three cells since a failure in cell a_4 is emulated (it is bypassed from that cluster). By comparing the output voltage depicted in Fig. 8 (before the failure), it is seen that voltages of the three phases are composed of nine levels. On the other

hand, from Fig. 9, it is appreciated that the voltage of cluster "a" (where the failure occurs), the voltage is composed just by seven levels. From these figures, it is concluded that even this critical situation, the distributed control scheme ensure a balanced output voltage for the STATCOM.

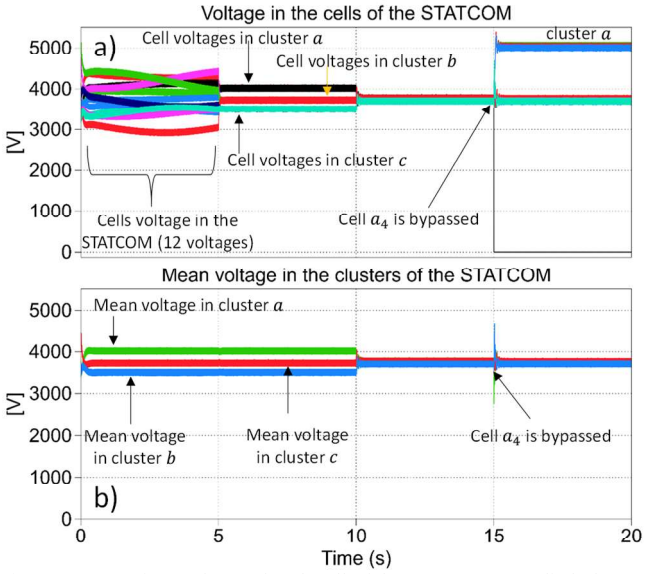

Fig. 6. (a) Capacitor' voltage of each cell of the STATCOM studied, (b) DC mean capacitor voltage in each cluster —both the initial voltage and capacitance of each cell are different. (Voltage around 3750V and capacitance around C)

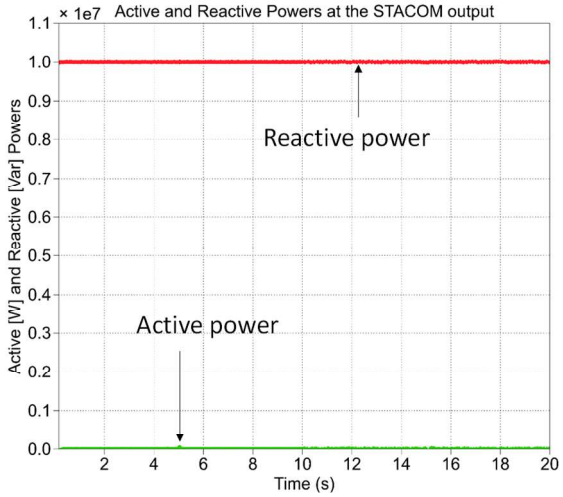

Fig. 7. Active and reactive power at the output of the STATCOM.

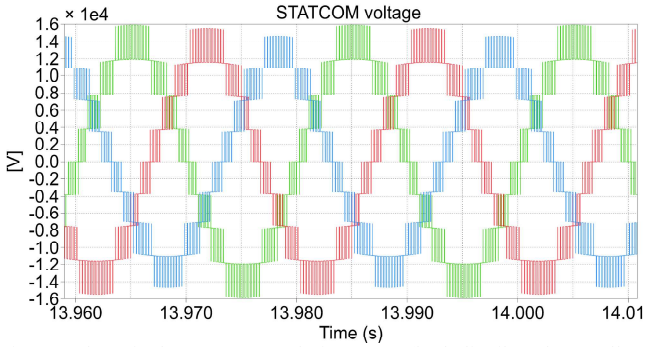

Fig. 8. Voltage in the STATCOM during step 3 (both distributed controllers are working) —All waveforms are generated with nine levels.

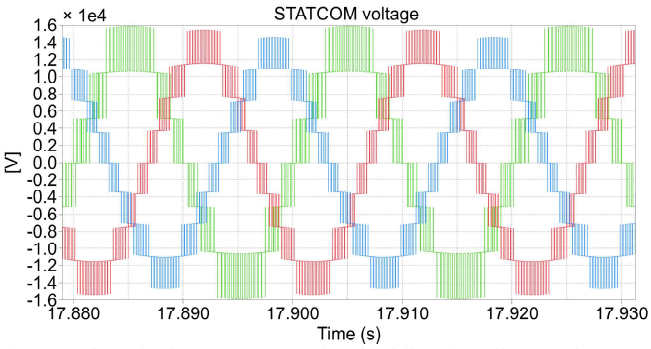

Fig. 9. Voltage in the STATCOM after the failure in cell a_4 —The green waveform (cluster a) is generated with seven levels.

B. Test scenario 2: Performance of the distributed controller in front of communication time delays in the communication network

To analyse the performance of the distributed controllers (13) and (14) in front of delays in the communication network, a communication time-delay τ is introduced, as shown in (17) and (18) respectively. This means, that the consensus algorithm (17) in cell "i" receives the information v_{x_j} from the rest of cells with a time-delay equal to τ. The similar occurs for the inter-cluster consensus algorithm (18). The performance of controllers is analysed for the following cases: $\tau = 0.1s$ and $\tau = 0.7s$.

$$v_{x_i}^{cell} = -\frac{k_p^{cell} \cdot i_x}{N} \sum_{j=1}^{N} h_{ij} \cdot \left(v_{x_i} - v_{x_j}(t-\tau)\right) \tag{17}$$

$$v_{Cx}^{cl} = -k_p^{cl} \cdot \frac{i_x}{3} \sum_{j=1}^{3} g_{xj} \cdot \left(v_{Cx} - v_{Cj}(t-\tau)\right) \tag{18}$$

At the beginning of this test, just the overall control system (see Fig. 5) is working to regulate v_C^* at 3750V and Q^* to 5MVA. Then, at t=5s, the inter-cell (17) and inter-cluster consensus algorithm (18) are simultaneously enabled. Finally, at the t=10s, the reactive power reference Q^* is changed to 10MVA.

Fig. 10(a) shows the cell voltage and Fig. 10(b) shows the mean DC voltage in the clusters; both traces are getting for a time-delay equal to 0.1s. Fig. 11 shows the same information but for a time-delay of 0.7s. From these figures, it is concluded that the consensus of voltages is achieved for the two cases considered in this test ($\tau = 0.1s$ and $\tau = 0.7s$). Note that, for the largest time-delay ($\tau = 0.7s$), the consensus is achieved after some oscillations. From this test, an excellent performance of the consensus algorithms (13) and (14) is concluded, in terms of time delays.

Finally, Fig. 12, shows both the active and reactive power for the case $\tau = 0.7s$. From this figure, it is concluded that even though the communication time-delay, the STATCOM is able to feed the system with reactive power.

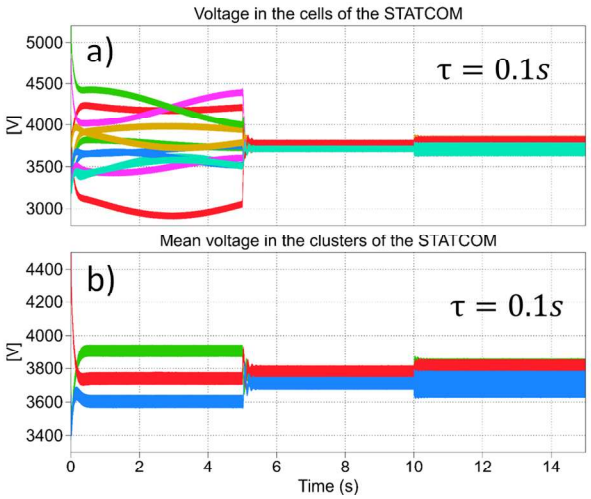

Fig. 10. (a) Cell voltage and (b) DC mean capacitor voltage in each cluster for a time-delay of 0.1—both the initial voltage and capacitance of each cell are different. (Voltage around 3750V and capacitance around C)

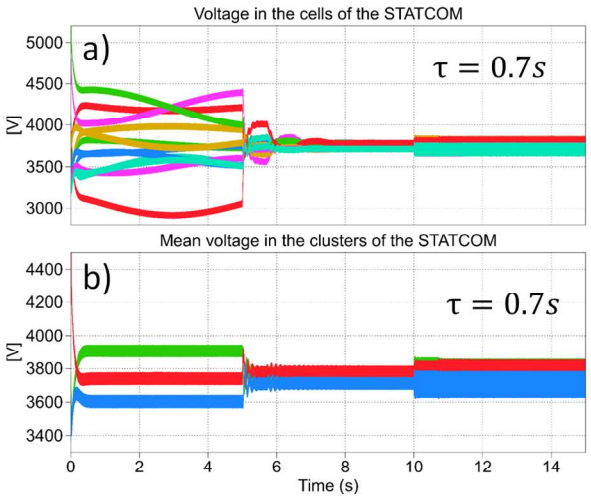

Fig. 11. (a) Cell voltage and (b) DC mean capacitor voltage in each cluster for a time-delay of 0.7s.

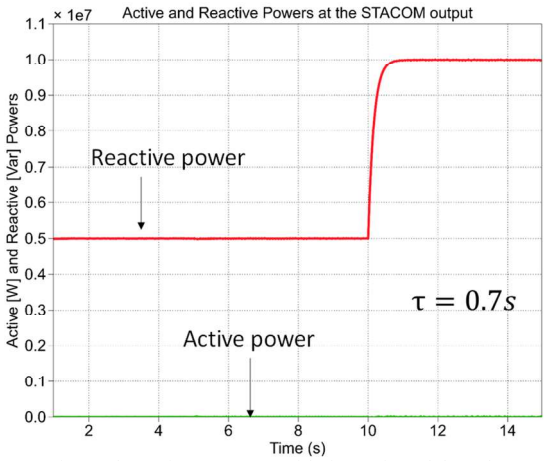

Fig. 12. Active and reactive power considering a time-delay of 0.7s.

C. *Test scenario 3: Performance of the distributed controller in front of failures on the communication network links*

In this test, the performance of the proposed consensus-based distributed control system is evaluated in front of failures in the communication links. At the beginning of this test, just the overall control system (see Fig. 5) is working to regulate v_C^* at 3750V and Q^* 5MVA. Then, at t=5s, the inter-cell (13) and inter-cluster consensus algorithm (14) are simultaneously enabled. It is worth remembering that in this case, the inter-cell communication topology is that given by the graph (a) in Fig. 5, and the inter-cluster communication topology is that shown by graph (d) on the top of Fig. 5. Afterwards, at t=10s, a communication link failure in both graphs is emulated. Fig. 13 and Fig. 14 show, respectively, the inter-cell and inter-cluster communication topologies before and after the communication link failure. Finally, at the t=15s, the reactive power reference Q^* is changed to 10MVA.

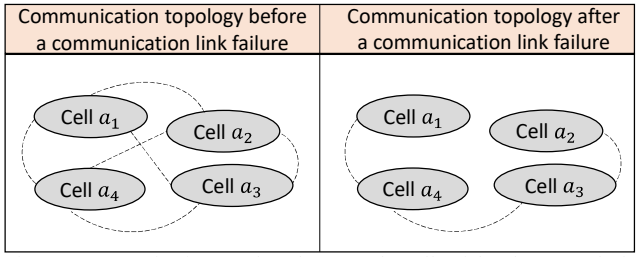

Fig. 13. Communication topology between the cells of the cluster "a" before and after a communication link failure. (The same communication link failure occurs in cluster "b" and "c")

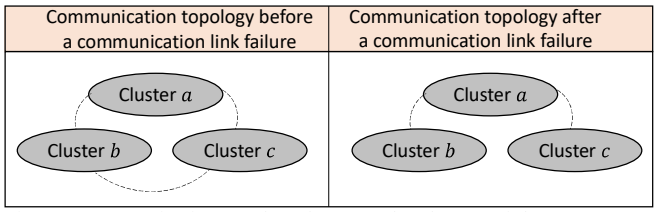

Fig. 14. Communication topology between the clusters of the STATCOM before and after a communication link failure.

Fig. 15 shows the cell voltage and the mean voltage in the clusters for this test. From this figure, it is concluded that the proposed consensus-based distributed controllers (13)-(14) works well even after the communication links failures. This demonstrates the effectiveness of the controller in terms of communication links failures. Finally, the injection of reactive power from the STATCOM to the system is not affected, as shown in Fig. 16.

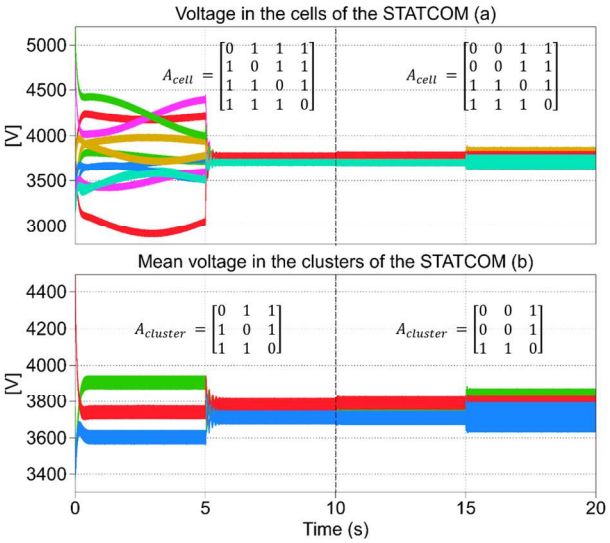

Fig. 15. (a) Cell voltage and (b) DC mean capacitor voltage in each cluster for the communication link failure test—both the initial voltage and capacitance of each cell are different.

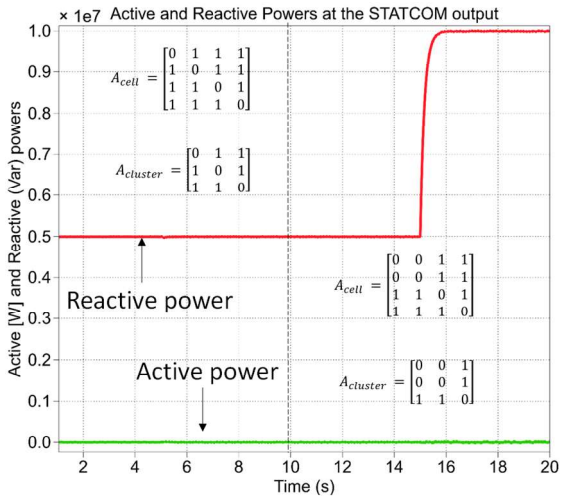

Fig. 16. Active and reactive powers for the communication link failure test.

V. CONCLUSIONS

Two consensus-based distributed controllers have been proposed and validated by simulation, one for balancing the inter-cell voltages, and the other one to control the inter-clusters mean-voltage in an MMCC STATCOM. The proposal was verified by considering the following cases: (i) performance of the control system front of a cell failure, (ii) the effects of communication time delays in the communication network, and (iii) performance of the controller in front of failures on the communication links. The performance of the consensus-based distributed controller was excellent. As future work, the experimental validation of the proposal along with its extension to be used in more complex control systems.

REFERENCES

[1] H. Akagi, "Classification, Terminology, and Application of the Modular Multilevel Cascade Converter (MMCC)," in IEEE Transactions on Power Electronics, vol. 26, no. 11, pp. 3119-3130, Nov. 2011, doi: 10.1109/TPEL.2011.2143431..

[2] H. Geng, S. Li, C. Zhang, G. Yang, L. Dong and B. Nahid-Mobarakeh, "Hybrid Communication Topology and Protocol for Distributed-Controlled Cascaded H-Bridge Multilevel STATCOM," *IEEE Transactions on Industry Applications,* vol. 53, no. 1, pp. 576 - 584, 2017.

[3] J. W. Simpson-Porco, Q. Shafiee, F. Dörfler, J. C. Vasquez, J. M. Guerrero and F. Bullo, "Secondary Frequency and Voltage Control of Islanded Microgrids via Distributed Averaging," *IEEE Transactions on Industrial Electronics,* vol. 62, no. 11, pp. 7025 - 7038, 2015.

[4] Y. Luo, Z. Li, Y. Li and P. Wang, "A distributed control method for power module voltage balancing of modular multilevel converters," in *2016 IEEE Energy Conversion Congress and Exposition (ECCE)*, Milwaukee, WI, USA, 2016.

[5] B. Xia, Y. Li, Z. Li, F. Xu and P. Wang, "A distributed voltage balancing method for modular multilevel converter," in *2017 IEEE 3rd International Future Energy Electronics Conference and ECCE Asia (IFEEC 2017 - ECCE Asia)*, Kaohsiung, Taiwan, 2017.

[6] J. Liu, W. Yao, Z. Lu and J. Ma, "Design and implementation of a distributed control structure for modular multilevel matrix converter," in *2018 IEEE Applied Power Electronics Conference and Exposition (APEC)*, San Antonio, TX, USA, 2018.

[7] P.-H. Wu, Y.-C. Su, J.-L. Shie and P.-T. Cheng, "A Distributed Control Technique for the Multilevel Cascaded Converter," *IEEE Transactions on Industry Applications,* vol. 55, no. 2, pp. 1649 - 1657, 2019.

[8] P. Poblete, J. Pereda, F. Nunez and R. P. Aguilera, "Distributed Current Control of Cascaded Multilevel Inverters," in *2019 IEEE International Conference on Industrial Technology (ICIT)*, Melbourne, Australia, Australia, 2019.

[9] G. Chen and Z. Guo, "Distributed Secondary and Optimal Active Power Sharing Control for Islanded Microgrids With Communication Delays," *IEEE Transactions on Smart Grid,* vol. 10, no. 2, pp. 2002 - 2014, 2019.

[10] J. Llanos, . D. E. Olivares, J. W. Simpson-Porco, M. Kazerani and D. Sáez, "A Novel Distributed Control Strategy for Optimal Dispatch of Isolated Microgrids Considering Congestion," *IEEE Transactions on Smart Grid,* vol. 10, no. 6, pp. 6595 - 6606, 2019.

[11] F. Guo, C. Wen, J. Mao and Y.-D. Song, "Distributed Economic Dispatch for Smart Grids With Random Wind Power," *IEEE Transactions on Smart Grid,* vol. 7, no. 3, pp. 1572 - 1583, 2016.

[12] L. Meng, X. Zhao, F. Tang, M. Savaghebi, T. Dragicevic, J. C. Vasquez and J. M. Guerrero, "Distributed Voltage Unbalance Compensation in Islanded Microgrids by Using a Dynamic Consensus Algorithm," *IEEE Transactions on Power Electronics,* vol. 31, no. 1, pp. 827 - 838, 2015.

[13] J. Zhou, S. Kim, H. Zhang, Q. Sun and R. Han, "Consensus-Based Distributed Control for Accurate Reactive, Harmonic, and Imbalance Power Sharing in Microgrids," *IEEE Transactions on Smart Grid,* vol. 9, no. 4, pp. 2453 - 2467, 2018.

[14] C. Burgos-Mellado, J. Llanos, R. Cárdenas, D. Sáez, D. E. Olivares, M. Sumner and A. Costabeber, "Distributed Control Strategy Based on a Consensus Algorithm and on the Conservative Power Theory for Imbalance and Harmonic Sharing in 4-Wire Microgrids," *IEEE Transactions on Smart Grid,* vol. 11, no. 2, pp. 1604 - 1619, 2020.

[15] C. Burgos-Mellado, J. L. E. Espina, D. Saez, R. Cardenas, M. Sumner and A. Watson, "Single-Phase Consensus-Based Control for Regulating Voltage and Sharing Unbalanced Currents in 3-Wire Isolated AC Microgrids," *IEEE Access,* vol. 8, pp. 164882 - 164898, 2020.

[16] S. Song and J. Liu, "Interpreting the Individual Capacitor Voltage Regulation Control of PSC-PWM MMC via Consensus Theory," *IEEE Access,* pp. 66807 - 66820, 2019.

[17] J. W. Simpson-Porco, Q. Shafiee, F. Dörfler, J. C. Vasquez, J. M. Guerrero and F. Bullo, "Secondary Frequency and Voltage Control of Islanded Microgrids via Distributed Averaging," *IEEE Transactions on Industrial Electronics,* vol. 62, no. 11, pp. 7025 - 7038, 2015.

[18] A. Bidran, V. Nasirian, A. Davoudi and F. L. Lewis, Cooperative Synchronization in Distributed Microgrid Control, Springer.

[19] F. L. Lewis, H. Zhang, K. Hengster-Movric and A. Das, Cooperative Control of Multi-Agent Systems: Optimal and Adaptive Design Approaches, Springer.

[20] R. Olfati-Saber and R. M. Murray, "Consensus problems in networks of agents with switching topology and time-delays," *IEEE Transactions on Automatic Control,* vol. 49, no. 9, pp. 1520 - 1533, 2004.

[21] J. I. Y. Ota, Y. Shibano and H. Akagi, "A Phase-Shifted PWM D-STATCOM Using a Modular Multilevel Cascade Converter (SSBC)—Part II: Zero-Voltage-Ride-Through Capability," *IEEE Transactions on Industry Applications,* vol. 51, no. 1, pp. 289-296, 2015.

[22] H. Akagi, S. Inoue and T. Yoshii, "Control and Performance of a Transformerless Cascade PWM STATCOM With Star Configuration," *IEEE Transactions on Industry Applications,* vol. 43, no. 4, pp. 1041 - 1049, 2007.

[23] J. I. Y. Ota, Y. Shibano, N. Niimura and H. Akagi, "A Phase-Shifted-PWM D-STATCOM Using a Modular Multilevel Cascade Converter (SSBC)—Part I: Modeling, Analysis, and Design of Current Control," *IEEE Transactions on Industry Applications,* vol. 51, no. 1, pp. 279 - 288, 2015.